

Kinetics of DNA-coated sticky particles

Kun-Ta Wu,¹ Lang Feng,¹ Ruojie Sha,² Rémi Dreyfus,³ Alexander Y. Grosberg,¹ Nadrian C. Seeman,² and Paul M. Chaikin¹

¹*Center for Soft Matter Research, New York University, New York, New York, USA*

²*Chemistry Department, New York University, New York, New York, USA*

³*Complex Assemblies of Soft Matter, CNRS-Rhodia-UPenn UMI 3254, Bristol, Pennsylvania 19007, USA*

(Received 16 October 2012; revised manuscript received 13 June 2013; published 12 August 2013)

DNA-functionalized particles are promising for complex self-assembly due to their specific controllable thermoreversible interactions. However, there has been little work on the kinetics and the aggregation rate, which depend on the rate of particle encounters and the probability that an encounter results in particles sticking. In this study, we investigate theoretically and experimentally the aggregation times of micron-scale particles as a function of DNA coverage and salt concentration. Our 2- μm colloids accommodate up to 70 000 DNA strands. For full coverage and high salt concentration, the aggregation time is 5 min while for 0.1 coverage and low salt it is 4 days. A simple model using reaction-limited kinetics and experimental oligomer hybridization rates describes the data well. A controlling factor is the Coulomb barrier at the nanometer scale retarding DNA hybridization. Our model allows easy measurements of microscopic hybridization rates from macroscopic aggregation and enables the design of complex self-assembly schemes with controlled kinetics.

DOI: [10.1103/PhysRevE.88.022304](https://doi.org/10.1103/PhysRevE.88.022304)

PACS number(s): 82.70.Dd, 81.16.Dn, 87.14.gk

I. INTRODUCTION

DNA-functionalized colloids have gained interest because DNA hybridization gives colloids highly selective thermoreversible attractions [1,2]. Rapid developments in DNA technology now allow facile synthesis of specifically designed DNA sequences easily linked to particle surfaces. Recently, ordered Face-Centered Cubic (FCC) crystalline structures from a single component system and Body-Centered Cubic (BCC) crystals from two different colloids coated with complementary DNA “sticky ends” (DNA single strands) have been made [3–5]. This considerable achievement in the self-assembly field allows us to envision more complex multistage processes such as self-assembly of clusters [6] or self-replication at the colloidal scale [7]. For such multistep processes, thermodynamics controls the structure of the intermediate product at each stage, whereas the kinetics controls the time it takes to form the intermediate product. Models to describe the thermodynamics of particle aggregation with varying DNA particle coverage have been successfully developed and compared to experimental data [2,3,7–14]. However, the mechanism of particle pair formation and the kinetics of aggregation remains poorly studied. This work also bears on others sticky particles using, e.g., proteins.

II. SYSTEM DESCRIPTION

The system under investigation is a mixture of two populations of colloids: one population is coated with a DNA strand (S), and the other is coated with the complementary strand (S'). When these two populations of colloids are mixed together at low temperature, they form aggregates due to the hybridization of S and S'. We have studied the aggregation kinetics and how it is affected by DNA surface coverage and salt concentration. The number of active DNA strands on a particle is varied from $\sim 70\,000$ (full coverage) to ~ 1750 . Salt concentration, [NaCl], is increased from 0 to 200 mM. We find that the particle aggregation kinetics is controlled by the interplay

particle diffusion and DNA sticky-ends hybridization. The time two colloidal particles remain within an interaction region of distance determined by the length L of the DNA constructs [see Fig. 1(a)] is found to be $\tau_c \approx 30$ ms [15,16]. The competing time is τ_h , the hybridization time for one pair of sticky ends when particle surfaces are within a distance $2L$. If the number of possible bonding configurations is N_G , then for $\tau_c \gg \tau_h/N_G$, aggregation is diffusion limited. For $\tau_c \lesssim \tau_h/N_G$, aggregation is reaction limited. Of particular interest in our study is the effect of added salt. Although the Debye screening length, λ , varies only from 1.6 to 0.6 nm [17,18], i.e., it remains much smaller than both the particle radius $R_p \approx 980$ nm and DNA length $L \approx 16.8$ nm, the aggregation rate varies over a factor of 300 as salt concentration is varied (see Fig. 3). This results from a Coulomb energy barrier between hybridizing DNA backbones. Thus, we can infer from the measurement of the aggregation time on a microscopic scale the strength of this energy barrier on a nanoscale.

III. EXPERIMENT

A. Particle characterization

A schematic illustration of our experimental system is shown in Fig. 1(a). Our particles are streptavidin-coated polystyrene particles (Streptavidin Microspheres, 2 μm , Polyscience, Inc., 1.25% polydispersity). Our DNA constructs consist of a 61-nucleotide oligomer (IDT, Coralville, IA), attached via a short poly (ethylene glycol) spacer to a 5' biotin group and hybridized from its 5' end to 49-nucleotide complementary strands (CS). DNA is purified by polyacrylamide gel electrophoresis (PAGE) before being coated on the particles. In our experiments, we use three kinds of DNA. Two of them (S and S') are complementary to each other on the 3' end. The third, “neutral,” DNA (N) only has 11 bases of thymine on the 3' end. The particles are coated with DNA S(S') and DNA N in the ratio $\chi = n_{S(S')}/[n_{S(S')} + n_N]$, where $n_{S(S')}$ and n_N are respectively the number of DNA

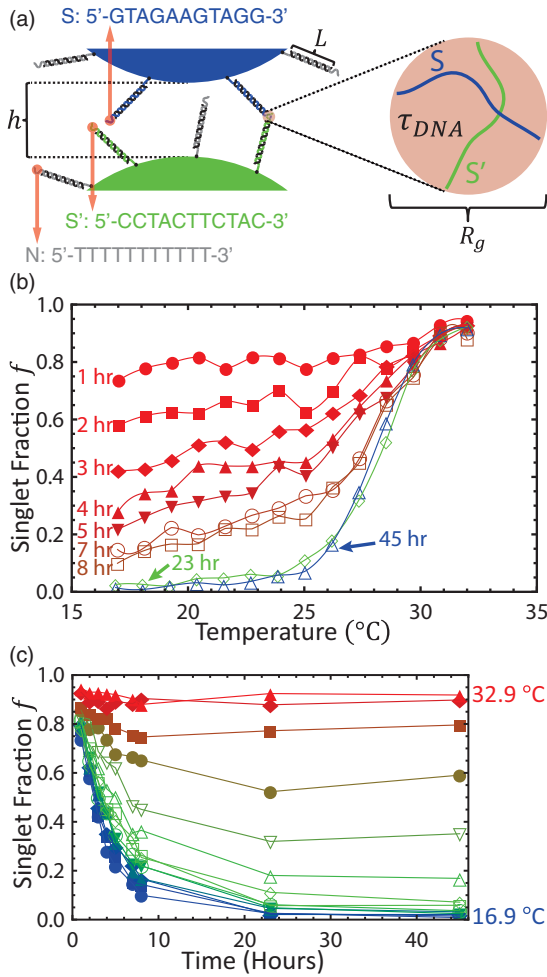


FIG. 1. (Color online) (a) Schematic representation of the system. The aggregation kinetics relates to the microscopic hybridization time of single DNA strands S and S'. (b) Time evolution of the singlet fraction vs temperature for a surface coverage of 1 DNA per (59 nm)², $\chi = 0.05$. (c) Same data as in (b) plotted as singlet fraction vs time for different temperatures.

S(S') and DNA N per particle [10–12]. For $\chi = 1$ the surface coverage is 1 active DNA/(13 nm)². To stabilize the particles, experiments are performed in buffer containing surfactants: 10 mM phosphate-buffered saline (PBS), 50 mM NaCl, 0.15% w/w sodium lauryl sulfate (SDS), and 0.5% w/w pluronic F127, in a capillary (0.2 mm in height, 2 mm in width, and 5 cm in length). Experiments with noncomplementary particles at twice the concentration of SDS and F127 show no signs of depletion interactions in the entire temperature and concentration range studied.

The aggregation develops as essentially a two-dimensional (2D) process, since our particles reside within a gravitational height $\sim k_B T / \Delta m g \approx 2.2 \mu\text{m}$, about particle diameter, from the cell bottom ($k_B T$ is thermal energy). The 2D concentration of particles is $C_p = 0.01 \text{ particle}/\mu\text{m}^2$.

B. Measurements of aggregation times

To measure the melting curves and the time-dependent behavior of particle aggregation our sample is placed on

a temperature gradient stage on a light microscope (see Appendix A). To quantitatively characterize colloidal aggregation, we measured the fraction of nonaggregated particles or the “singlet fraction.” Since the system is basically two-dimensional, we can determine the singlet fraction by (1) taking an image of colloids, (2) identifying single particles and particle aggregates by their area, and (3) the singlet fraction of the image $f \equiv \text{areas of single particles}/\text{total areas of particles}$ [10–12]. Therefore, we can monitor $f(T)$ as a function of time at different distances along the gradient until $f(T)$ is independent of time. The results for $\chi = 0.05$ are shown in Fig. 1(b). Similarly, we can find how $f(T)$ decays with time at several temperatures, as shown in Fig. 1(c). Note that for fixed coverage, χ , the characteristic time to form an equilibrium singlet fraction is approximately independent of temperature, Fig. 1(c). The experiment was performed for $\chi = 0.025, 0.05, 0.1, 0.2, 0.3, 0.4, 0.5, 0.75, \text{ and } 1$. The corresponding melting temperatures T_m 's, defined as $f(T_m) \equiv 0.5$, are 22 °C, 28.4 °C, 34.5 °C, 41.5 °C, 44.3 °C, 45.4 °C, 46.9 °C, 48.3 °C, and 50.3 °C.

The singlet fraction as a function of time for each χ is shown in Fig. 2(a). For each χ the temperature is chosen to be low enough for particles to fully aggregate, i.e., $f(T, t)$ approaches

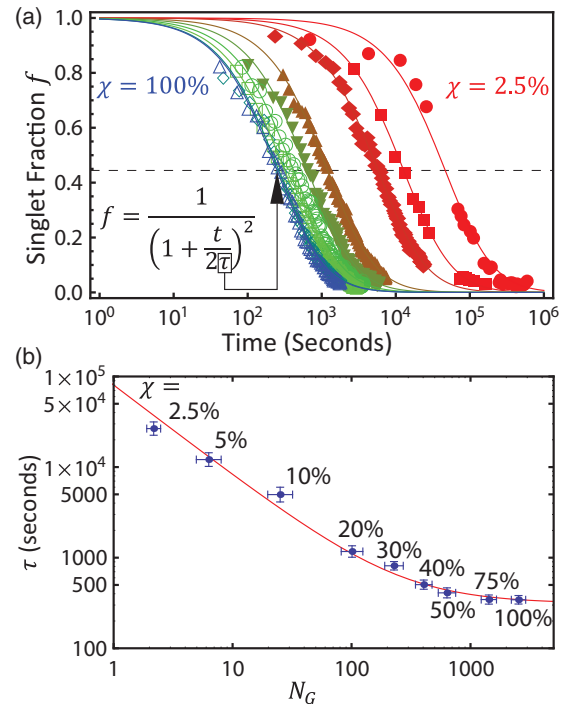


FIG. 2. (Color online) (a) Singlet fraction vs time for each sticky-end DNA coverage ratio χ at a corresponding fixed temperature. From left (blue) to right (red), $\chi = 1, 0.75, 0.5, 0.4, 0.3, 0.2, 0.1, 0.05, \text{ and } 0.025$ respectively. The corresponding temperatures are 42 °C, 40 °C, 38 °C, 36 °C, 36 °C, 33 °C, 25 °C, 22 °C, and 12 °C respectively. The solid curves are the fit curves from Eq. (1). The intersection of the dashed line and the solid curve indicate the characteristic aggregation time τ . (b) The characteristic aggregation time τ vs. possible bonding configurations N_G . The blue dots are the experimental data. The red curve is determined by Eq. (9) with $\lambda = 1 \text{ nm}$, $\tau_{DLA} = 313 \text{ s}$, and $\tau_{DNA}^{(0)} = 230 \mu\text{s}$.

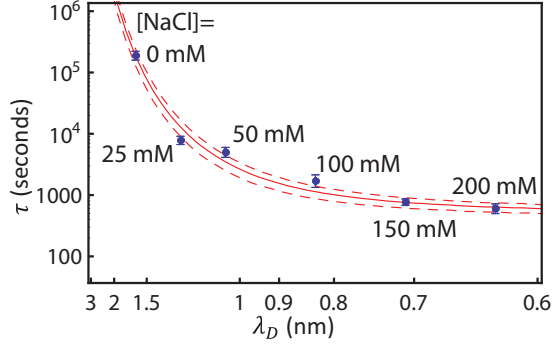


FIG. 3. (Color online) The characteristic aggregation time τ vs Debye Hückel screening length λ_D for $\chi = 0.1$. The blue dots are the experimental data. The red curve is determined by Eq. (9) with $\chi = 0.1$, equivalently $N_G = 25$. The dashed curves indicate the uncertainty of the model due to the uncertainties of τ_{DLA} , $\tau_{DNA}^{(0)}$, χ , and total DNA coverage on the particles.

zero as $t \rightarrow \infty$. Typically we choose T to be $\sim 8^\circ\text{C}$ below T_m . To understand the results presented in Fig. 2(a), we consider the “chemical” reaction: $n_i + n_j \xrightleftharpoons[k_{ij}^{\text{off}}]{k_{ij}^{\text{on}}} n_k$, where n_i indicates the number density of clusters with i particles, while k_{ij}^{on} and k_{ij}^{off} are the association and dissociation rates respectively. In the low-temperature regime in which we are working, we can assume $k^{\text{off}} \rightarrow 0$. This is then the classical Smoluchowski coagulation [19,20], with functional form and characteristic time expressed as follows:

$$f(t) = \frac{n_1(t)}{C_p} = \frac{1}{\left(1 + \frac{t}{2\tau}\right)^2}, \quad \tau = \frac{1}{k^{\text{on}}C_0}. \quad (1)$$

Here $C_0 = C_p/2 = 0.005$ particles/ μm^2 is the concentration of particles of one particular type, i.e., coated with either DNA S or S'. Equation (1) provides an excellent fit to our data, as indicated by solid lines in Fig. 2(a), which allows us to extract a characteristic aggregation time τ for each χ by defining $f(t = \tau) = 4/9$. Our measured τ increases from 5 min for $\chi = 1$ to 11 h for $\chi = 0.025$ [see Fig. 2(b)] [21]. Furthermore, we performed experiment at $\chi = 0.1$ for salt concentrations ranging from $[\text{NaCl}] = 0$ to 200 mM [18], and the fit of Eq. (1) to the data (not shown) remains excellent. The characteristic aggregation time τ increases from 7.3 min for 200 mM to 79 h for 0 mM (see Fig. 3).

IV. MODEL

A. Two-dimensional reaction rates

To gain an insight into the nature of aggregation time τ and its sharp dependence on salt, we consider a steady 2D diffusion of particles along the cell bottom. We impose a reaction boundary condition [22,23] to account for the fact that our particles may diffuse into and out of a reaction region before the sticky ends have time to hybridize (which corresponds to the crossover from diffusion-limited to reaction-limited

aggregation [24,25]):

$$\begin{aligned} \frac{1}{r} \frac{d}{dr} \left[r \frac{d}{dr} C(r) \right] &= 0 \quad \text{stationary process} \\ 2D \frac{d}{dr} C|_{2R_p} &= \frac{1}{\tau_r} LC|_{2R_p} \quad \text{boundary condition} \quad (2) \\ \int_{2R_p}^{\frac{1}{\sqrt{\pi c_0}}} 2\pi r C(r) dr &= 1 \quad \text{normalization,} \end{aligned}$$

where τ_r is the reaction time of a pair of particles with complementary sticky-end DNA on their surfaces staying within the reaction region (thickness L). The solution of Eqs. (2) gives the spatial dependence of the particle concentration $C(r)$, the rate of particle aggregation from Fick’s law k^{on} , and the aggregation time τ (see Appendix B),

$$\tau = \tau_{DLA} + \frac{\tau_r}{4\pi R_p LC_0}, \quad (3)$$

where

$$\tau_{DLA} \equiv \frac{-\ln(4\pi e R_p^2 C_0)}{8\pi DC_0}. \quad (4)$$

In our case, $\tau_{DLA} \approx 70$ s. For $\tau_r \rightarrow 0$, the result is two-dimensional diffusion-limited aggregation (DLA). This is equivalent to setting $C|_{2R_p} = 0$ in the second of Eqs. (2) where each collision leads to aggregation.

B. Number of bonding configurations N_G

We here are mostly interested in the deviations from Smoluchowski DLA, coming from a finite value of τ_r : These are enhanced by slow hybridization of the sticky ends and reduced by the number of possible bonding configurations N_G . We assume that $N_G \approx g_b N_b$, where N_b is the number of DNA strands in an accessible patch on a particle and g_b is the number of complementary DNA strands on a particle accessible to a DNA strand on the corresponding opposing particle [10–12]. In our case, $N_b \approx 300$ and $g_b \approx 9$ for full coverage and a particle surface separation of $h = 16.8$ nm.

For a particle of radius R_p , with a surface separation of h from a neighboring particle, $N_b \approx \rho A$, with ρ the surface DNA strand density, and $A \approx \pi R_p(2L - h)$, the area of a patch from which strands can bridge between the particles. With these approximations $N_b \approx \pi R_p(2L - h)\rho$ and $g_b \approx \pi\rho(4L^2 - h^2)$ [10–12]. For less densely coated particles, we obtain a value of N_b and g_b by simulation [12]. We randomly distribute $4\pi R_p^2\rho$ strands homogeneously on a particle surface and count N_b and g_b with a similarly prepared particle at the surface separation of a distance h . After determining N_b and g_b , we can approximate $N_G \approx g_b N_b$.

Knowing N_G , we determined $\tau_r \approx \tau_h/N_G$, where τ_h is the hybridization time for one pair of sticky ends. It is this τ_h that is crucial, because it depends on the salt.

C. Rotational search time for DNA strands

We now want to relate τ_h , the hybridization time of the sticky ends on our DNA constructs, to τ_{DNA} , the hybridization time for two complementary oligomers with the same sequence as our sticky ends if they were contained in a volume of length scale of their own radius of gyration, R_g [see R_g in Fig. 1(a)].

This problem is somewhat similar to the previous one, because hybridization can be either diffusion or reaction limited. Indeed, every sticky end diffuses, with angular or rotational diffusion constant, $D_\theta = k_B T / 8\pi\eta L^3$ (η is solvent viscosity), along a hemisphere of area $\sim 2\pi L^2$ at the end of rigid double-stranded DNA of length L attached to the particle surface [Fig. 1(a)]. The problem of binding two sticky ends from opposing particles is similar to the attachment of patches on two hemispheres of radius L held in contact but allowed to rotationally diffuse [26,27]. From Ref. [26], we know that the time for a ligand and a receptor to meet each other by rotational diffusion is mostly determined by the relative capture surface, which is the ratio of the area of the ligand or receptor and the surface area of the sphere as shown in Fig. 4(a). Similarly, in our case, as shown in Fig. 4(b), since DNA sticky ends only can be hybridized together when they are both in the red area, we can adapt the concept of Fig. 4(a) to Fig. 4(b). We can find that the time for a pair of complementary sticky ends to meet each other by the rotational diffusion of their dsDNA backbones can be estimated as $D_\theta^{-1} \ln 4/\alpha$ [see Eq. (14) of Ref. [26]], where

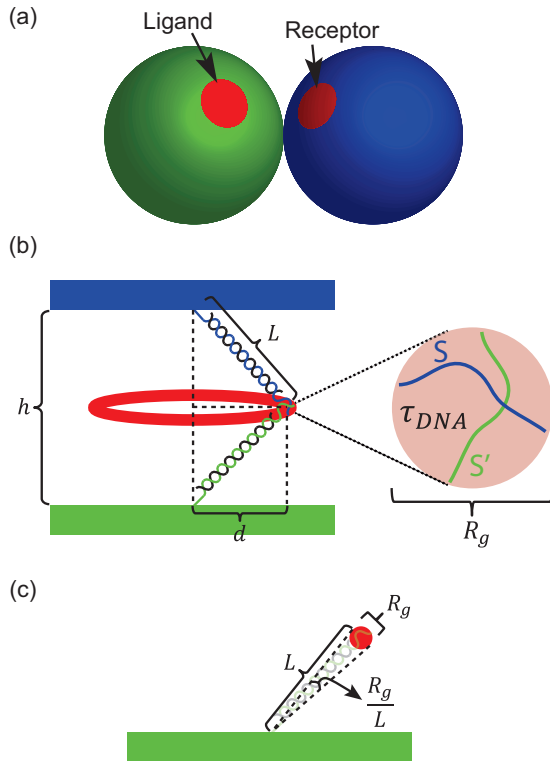


FIG. 4. (Color online) (a) A pair of spheres with reaction patches held in contact. The red patches are a ligand for the green sphere (left) and a receptor for the blue sphere (right). The two spheres are held in contact and are allowed to rotational diffuse. The ligand-receptor reaction will be triggered when the ligand and the receptor touch each other by the rotational diffusion of the spheres. (b) A pair of complementary DNA strands attached to colloidal surfaces. Since the backbones of the DNA strands can rotate freely, the spatial diffusion space of the each sticky end is the surface of a hemisphere with a radius L . The overlapping area of the two hemispheres is the red ring. These two DNA sticky ends can only hybridize when they are both in the ring. Hence, the ring is like the reaction patch in (a). (c) The angle for the sticky end to rotationally diffuse its own size.

our relative capture surface $\alpha \equiv (2\pi d R_g)/(2\pi L^2)$, in which $2\pi d R_g$ is the red area and $2\pi L^2$ is the surface area of the hemisphere. For each pair of complementary DNA strands, d depends on the distance between them. If the base distance between a pair of DNA strands is h , then $d = \sqrt{L^2 - (h/2)^2}$. If the base distance between a pair of DNA strands is $2L$, then $d = 0$. Hence, $\sqrt{L^2 - (h/2)^2} \geq d \geq 0$. For a good estimate of the average of α , we choose $\bar{\alpha} \approx (2\pi \bar{d} R_g)/(2\pi L^2)$, where $\bar{d} \equiv \frac{1}{2}\sqrt{L^2 - (h/2)^2} \approx 7.2$ nm. Putting all the above equations and parameters together, we can estimate the rotational search time τ_s as

$$\tau_s \approx \frac{1}{D_\theta} \ln 4/\bar{\alpha} \approx \frac{1}{D_\theta} \ln 4 \frac{2\pi L^2}{2\pi \bar{d} R_g} = \frac{L^2 \ln 4}{D_\theta \bar{d} R_g}. \quad (5)$$

D. Rotational transit time

By following the same logic of estimating colloidal aggregation time τ , which needs colloidal diffusion time τ_{DLA} , colloidal collision time τ_c , and colloidal reaction time τ_r , we need to further estimate the collision time or, to distinguish the term usage from colloids, the rotational transit time for DNA strands, τ_θ . As shown in Fig. 4(c), once a pair of DNA sticky ends encounter each other by rotational diffusion of their dsDNA backbones, they will stay within binding range until they diffuse apart or until hybridization occurs. Hence, the rotational transit time τ_θ is the time for the pair of DNA to relatively diffuse a solid angle $\sim (R_g/L)^2$, which gives

$$\tau_\theta \approx \frac{1}{8D_\theta} \left(\frac{R_g}{L} \right)^2. \quad (6)$$

In our case, $\tau_\theta \approx 0.1 \mu\text{s}$.

E. Intrinsic DNA hybridization time

For a pair of complementary DNA strands to hybridize if they are held within their gyration radius R_p , they need to undergo a period of time τ_{DNA} . Hence, similarly, if $\tau_\theta \gg \tau_{\text{DNA}}$, DNA hybridization is diffusion limited. If $\tau_\theta \lesssim \tau_{\text{DNA}}$, DNA sticky ends need to undergo several encounters before they can hybridize. By following such logic along with the previously estimated rotational searching time and transit time for DNA sticky ends, we can easily estimate the hybridization time of the sticky ends on our constructs, τ_h as

$$\begin{aligned} \tau_h &\approx \text{rotational search time} \times (1 + \text{encounters needed}) \\ &\approx \frac{L^2 \ln 4}{D_\theta \bar{d} R_g} \left(1 + \frac{\tau_{\text{DNA}}}{\tau_\theta} \right). \end{aligned} \quad (7)$$

τ_{DNA} is now salt dependent due to the electrostatic repulsion between DNA strands which forms a barrier to hybridization,

$$\tau_{\text{DNA}} = \tau_{\text{DNA}}^{(0)} e^{U(\lambda)/k_B T}, \quad (8)$$

where $U(\lambda)$ is the energy barrier for a pair of complementary DNA strands to hybridize from being infinitely apart and λ is Debye screening length [17]. Combining Eqs. (3), (4), (7), and (8), our kinetic model then takes a final form as follows:

$$\tau \approx \tau_{\text{DLA}} \left\{ 1 + A \left[1 + \frac{\tau_{\text{DNA}}^{(0)} e^{U(\lambda)/k_B T}}{\tau_\theta} \right] \right\}, \quad (9)$$

where

$$A \equiv \frac{4DL \ln 2}{N_G D_\theta R_p R_g \bar{d} \ln \frac{1}{4\pi\epsilon R_p^2 C_0}}, \quad (10)$$

which can be interpreted as the ratio of binding time to resident time in a binding region.

F. Energy barriers of hybridization

To use Eq. (9), the barrier $U(\lambda)$ has to be quantified. However, there are few studies of this barrier [28–32]. For the sake of estimate, we model this barrier very crudely, as a screened Coulomb repulsion,

$$U(\lambda) \approx \frac{Q^2}{4\pi\epsilon\epsilon_0} \frac{1}{a} e^{-\frac{a}{\lambda}}, \quad (11)$$

between two charges Q a distance a apart [33]. We take $a \approx 2.5$ nm, about the diameter of dsDNA. The value of effective charge Q is a more delicate issue. The full charge of sticky ends in our experiment is $-11q$; however, some fraction of it must be compensated by Manning condensation [34]. The exact compensated fraction is difficult to determine, because the very concept of condensation is questionable for ssDNA, and, moreover, we need the amount of condensation at the top of the barrier, when DNA is neither single nor double stranded. For the curves shown in Fig. 3 we assume no Manning condensation. A very similar curve results if we take the actual positions of 11 singly charged phosphate groups along with a screened interaction or if we accept a 0.25 Manning condensation, $Q = -11 \times (0.75q)$, and fit $a = 2$ nm [33]. Furthermore, once $U(\lambda)$ is determined, the hybridization time at high salt, when electrostatics is well screened, can be estimated from the literature: $\tau_{\text{DNA}}^{(0)} \approx 230 \mu\text{s}$ [26,31,32,35,36].

V. COMPARISONS OF EXPERIMENTS AND MODELS

After collecting the last ingredient, $U(\lambda)$, we are able to use our kinetic model, Eq. (9), for comparison with experiments. The most sensitive variables in our model are the particle coverage dependence of N_G and the salt dependence of $U(\lambda)$. Figure 2(b) shows the relation between τ and N_G . Although the variable in our experimental study is the particle coverage, we are able to determine the value of N_G for every particle coverage based on geometry considerations. Therefore, the agreement between experiment and model indicates both that the model is reasonable and that we have a good handle on evaluating N_G from geometry. We apply Eq. (9) to the data in Fig. 2(b) by setting $\lambda = 1$ nm and treating τ_{DLA} and $\tau_{\text{DNA}}^{(0)}$ as the fitting parameters. The fitting results are $\tau_{\text{DLA}} = (313 \pm 27)$ s and $\tau_{\text{DNA}}^{(0)} = (230 \pm 50) \mu\text{s}$.

For τ_{DLA} , the experimental result is almost 5 times larger than the calculation [see Eq. (4)]. This discrepancy can be explained by the fact that the experimental system is not really 2D. Particles can diffuse in the third dimension limited by an exponential atmosphere profile at the gravitational height. The result is a longer diffusion-limited aggregation time than an ideal 2D system.

For $\tau_{\text{DNA}}^{(0)}$, we do not have theoretical estimate, but we compare our experimental result with measurement data

available in literature, which is about $230 \mu\text{s}$ [26,31,32,35,36]. We found complete consistency of these results.

In Fig. 3, we show measurements of [NaCl] dependence of the aggregation time τ and a comparison with our model. Having fixed τ_{DLA} and $\tau_{\text{DNA}}^{(0)}$ there remain no adjustable parameters in the predicted behavior. Together Fig. 2(b) and Fig. 3 show remarkable agreement of experiments with our simple model.

VI. CONCLUSIONS

In conclusion, the kinetics of aggregation of sticky particles and in particular their aggregation rate is reduced from the conventional diffusion-limited result by a kinetic factor of $\frac{\tau_c}{\tau_h/N_G}$. A particle diffuses into and out of a reaction zone in time τ_c and must make many additional attempts if the reaction time $\tau_h/N_G > \tau_c$. This represents a well-known crossover to reaction-limited aggregation [24,25]. We show that a simple model appropriate for DNA-functionalized particles quantitatively describes the phenomena. These results are important for understanding aggregation and crystallization of functionalized colloids. Further, they are useful in designing and optimizing more complex self-assembly processes involving many steps of reversible and irreversible binding. There is also much current interest in the kinetics of DNA hybridization and the binding of proteins and other molecular and nanoscale constructs. Typically, these reactions occur on a $10^{-6} \sim 10^{-3}$ s time scale. Using our results, particles coated with these ligands substituted for the DNA can conveniently be studied on a minutes-to-hours time scale with simple microscopic observation or by dynamic light scattering.

ACKNOWLEDGMENTS

We acknowledge partial support from National Aeronautics and Space Administration under Grant No. NNX08AK04G and the Materials Research Science and Engineering Center under Grant No. DMR-0820341 for particle development and characterization. N.C.S. acknowledges support from National Institutes of Health Grant No. GM-29554 for DNA synthesis and characterization, and K.-T.W., L.F., and P.M.C. acknowledge support for thermal and optical data and analysis from Department of Energy-Basic Energy Sciences Grant No. DE3C0007991.

APPENDIX A: SETUP OF TEMPERATURE GRADIENT

A schematic diagram of our temperature gradient setup is shown in Fig. 5(a). Our sample is placed on a copper plate. Each of the ends of the copper plate are connected to a peltier, which is attached to the microscope stage. The microscope stage is specially made of metal with an internal liquid circulation system through which we flow water from a temperature-controlled bath. The two ends of the sample are attached to thermal sensors, which are connected to a temperature controller. One peltier is controlled by the temperature controller. The other peltier is connected to a dc power supply. The power supply and the temperature controller are both computer controlled. We use the proportional-integral-derivative algorithm (PID) to control cooling and heating

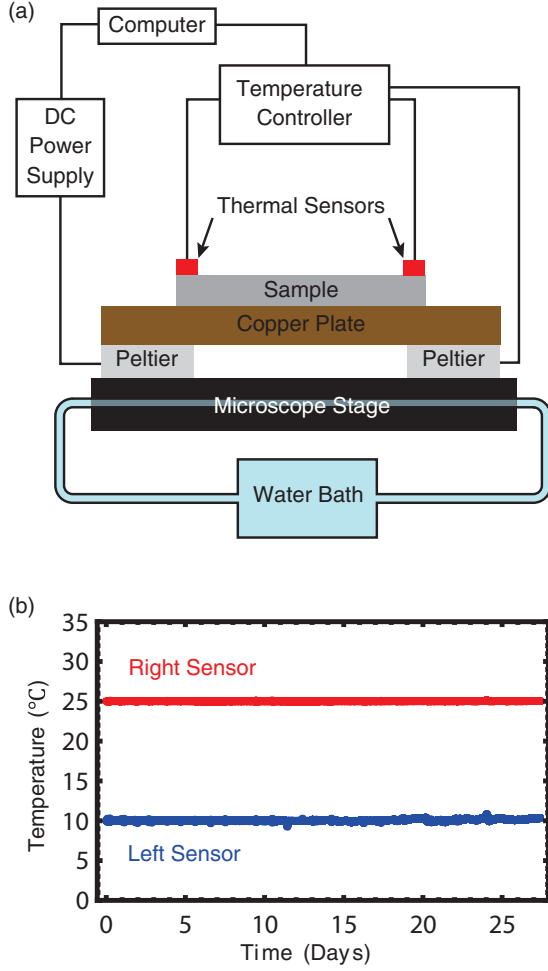


FIG. 5. (Color online) (a) The schematic diagram of our temperature gradient setup. (b) Monitored temperatures through a 27-day experiment. The upper (red) dots and lower (blue) dots are the temperatures measured through the right sensor and the left sensor as a function of time respectively. Over the period of 27 days, the averages of the measured temperatures from the left sensor and the right sensor are $(10.1 \pm 0.1)^\circ\text{C}$ and $(25 \pm 0.01)^\circ\text{C}$, respectively.

[37] on the dc supply. The computer monitors temperatures throughout the experiment are shown in Fig. 5(b). Typically, the fluctuations of temperatures measured through either the left sensor or the right sensor are about 0.1°C . In Fig. 5(b), the averages of the higher (red) and lower (blue) temperatures measured through a 27-day experiment are $(10.1 \pm 0.1)^\circ\text{C}$ and $(25 \pm 0.01)^\circ\text{C}$ respectively. Using the PID on one side and the temperature controller on the other, we are able to create a temperature gradient which lasts for months and is stable.

APPENDIX B: TWO-DIMENSIONAL COLLOIDAL AGGREGATION RATES

Our treatment follows the usual aggregation formulation of Refs. [19,20] but for two dimensions rather than the usual three. Colloidal aggregation can be categorized into two regimes: diffusion-limited aggregation (DLA) and reaction-limited aggregation (RLA). In the diffusion-limited case, the reaction rate, $k_{\text{DLA}}^{\text{on}}$, is dominated purely by particle diffusion because particles get bound immediately once they touch each

other. For the reaction-limited case, the reaction rate, $k_{\text{RLA}}^{\text{on}}$ is dominated by the competition of particle diffusion coefficient D and particle reaction rate k_r , which is defined as the binding efficiency for a pair of particles during the collision. On the following, we will discuss the difference of the aggregation rate for two-dimensional DLA and RLA in the case of the dilute free particle concentration: $R_p^2 C_0 \ll 1$.

Since particles basically diffuse freely before colliding, the free particle concentration distribution $C(\mathbf{r})$ can be described by Fick's law as follows:

$$\frac{\partial}{\partial t} C = 2D \nabla^2 C, \quad (\text{B1})$$

where $2D$ is the relative diffusion coefficient for a pair of particles. Consider the stationary state $\frac{\partial C}{\partial t} = 0$, Eq. (B1) is reduced to the Poisson equation: $\nabla^2 C = 0$. Further, consider one particle stationary at O with a radius $2R_p$ and another point particle diffuses within the disk of radius $\frac{1}{\sqrt{\pi C_0}}$. Then $C(\mathbf{r}) = C(r)$. The Poisson equation can be expressed as

$$\frac{1}{r} \frac{d}{dr} \left[r \frac{d}{dr} C(r) \right] = 0 \quad (\text{B2})$$

with a normalization condition,

$$\int_{2R_p}^{\frac{1}{\sqrt{\pi C_0}}} dr 2\pi r C(r) = 1. \quad (\text{B3})$$

1. Diffusion-limited aggregation

For DLA, we know that $C(2R_p) = 0$. Equation (B2) then can be solved as

$$C(r) = c \ln \frac{r}{2R_p}, \quad (\text{B4})$$

where c is a constant and can be determined from the normalization condition [see Eq. (B3)] as

$$\frac{1}{c} = \frac{1}{2C_0} \left[-\ln(4\pi R_p^2 C_0) - 1 + 4\pi R_p^2 C_0 \right].$$

Since we only consider the case of the dilute particle concentration, $R_p^2 C_0 \ll 1$, we can estimate c as

$$\frac{1}{c} \approx \frac{1}{2C_0} \left[-\ln(4\pi R_p^2 C_0) - 1 \right].$$

Hence, the particle aggregation rate $k_{\text{DLA}}^{\text{on}}$ can be determined by

$$\begin{aligned} & \# \text{ of particles flowing into the inner boundary } (r = 2R_p) \\ & \text{ per unit time} \\ &= 2\pi(2R_p)(2D) \frac{d}{dr} C(2R_p) \\ &= 4\pi Dc \\ &= \frac{8\pi DC_0}{-\ln(4\pi R_p^2 C_0) - 1} \\ &\equiv k_{\text{DLA}}^{\text{on}} C_0. \end{aligned}$$

We then find that

$$k_{\text{DLA}}^{\text{on}} = \frac{8\pi D}{-\ln(4\pi R_p^2 C_0) - 1} \quad (\text{B5})$$

or

$$\tau_{\text{DLA}} = \frac{1}{k_{\text{DLA}}^{\text{on}} C_0} = \frac{-\ln(4\pi e R_p^2 C_0)}{8\pi D C_0}. \quad (\text{B6})$$

Here we derived Eq. (4). The well-known three-dimensional result is $\tau_{\text{DNA}} = \frac{1}{8\pi D C_0 R_p}$.

2. Reaction-limited aggregation

For the case of RLA, the boundary condition is, instead of $C(2R_p) = 0$,

$$2\pi(2R_p)(2D)\frac{d}{dr}C(2R_p) = k_r[L2\pi(2R_p)C(2R_p)]. \quad (\text{B7})$$

The left-hand side is the number of particles flowing into the inner boundary ($r = 2R_p$) per unit time or the number of binding reactions per unit time. The right-hand side is the number of particles in the reaction region, which has the reaction thickness L , times the reaction efficiency, k_r . Equation (B2) then can be solved as

$$C(r) = c' \ln\left(\frac{r}{2R_p}\right) + \frac{D}{R_p k_r L} c', \quad (\text{B8})$$

where c' is a constant and can be estimated from normalization condition [see Eq. (B3)] as

$$\frac{1}{c'} \approx \frac{1}{2C_0} \left\{ \left[-\ln(4\pi R_p^2 C_0) - 1 \right] + \frac{2D}{R_p k_r L} \right\}.$$

Similarly, we can find that

$$\begin{aligned} & \# \text{ of particles flowing into the inner boundary } (r = 2R_p) \\ & \text{ per unit time} \\ &= 2\pi(2R_p)(2D)\frac{d}{dr}C(2R_p) \\ &= 4\pi D c' \\ &= \frac{8\pi D C_0}{\left[-\ln(4\pi R_p^2 C_0) - 1 \right] + \frac{2D}{R_p k_r L}} \\ &\equiv k_{\text{RLA}}^{\text{on}} C_0. \end{aligned}$$

We then find that

$$k_{\text{RLA}}^{\text{on}} = \frac{8\pi D}{\left[-\ln(4\pi R_p^2 C_0) - 1 \right] + \frac{2D}{R_p k_r L}} \quad (\text{B9})$$

or

$$\tau_{\text{RLA}} = \frac{1}{k_{\text{RLA}}^{\text{on}} C_0} = \tau_{\text{DLA}} + \frac{\tau_r}{4\pi R_p L C_0}, \quad (\text{B10})$$

where $\tau_r \equiv 1/k_r$. Here, we derived Eq. (3).

Note that $k_{\text{RLA}}^{\text{on}}$ is reduced to $k_{\text{DLA}}^{\text{on}}$ as k_r approaches infinity. This is consistent with our intuition: the diffusion-limited aggregation can be considered the reaction-limited aggregation with the infinitely strong binding reaction.

APPENDIX C: LIST OF TIMES

Times	Definition	Time scales
τ_{DLA}	Time for diffusion-limited aggregation. The characteristic time for colloidal aggregation assuming particle stick as soon as they collide. From Smoluchowski $\tau_{\text{DLA}} = \frac{1}{8\pi D R_p C_0}$ for three dimensions. For two dimensions see Eq. (4) and Eq. (B6).	Minutes to hours
τ_{RLA}	Reaction-limited aggregation. Time for colloidal aggregation when particles must have several encounters before they stick. See Eq. (B10).	Hours to months
τ	Aggregation time for colloidal particles. $\tau = \tau_{\text{DLA}}$ if $\tau_c \gg \tau_r$. $\tau = \tau_{\text{RLA}}$ if $\tau_c \lesssim \tau_r$. See Eq. (1), Eq. (3), and Eq. (9).	Minutes to months
τ_c	Collision time. Time that diffusing particles remain within an interaction distance, a distance in which they can bind. In our case, it is the time for particles to diffuse a distance L . See Ref. [16].	10 ms to 100 ms
τ_r	Reaction time. Time for complementary colloidal particles to bind when they are held within an interaction distance, a distance in which they can bind. In our case, $\tau_r \approx \tau_h/N_G$ where N_G is the number of ways they can bind.	10 ms to 10 s
τ_h	Hybridization time. Time for a pair of complementary DNA strands on complementary particles to bind when the particles are held within an interaction distance, and distance in which binding can occur. See Eq. (7).	1 s to 10 s
τ_s	Rotational search time. Time for a pair of complementary DNA sticky ends on complementary particles to encounter each other as their ‘‘backbones,’’ double stranded DNA attached to the complementary surfaces, undergo rotational diffusion. See Eq. (5).	0.1 ms to 1 ms
τ_θ	Rotational transit time. Time that a pair of complementary sticky ends to stay within their interaction zone, roughly their gyration radius, before they diffuse away by the rotational diffusion of their ‘‘backbones.’’ See Eq. (6).	0.1 μs
τ_{DNA}	Hybridization time for a pair of DNA ‘‘sticky ends’’ when they are held within their gyration radius R_g . Here we consider just the ‘‘sticky ends’’ not attached to any construct or surface freely diffusing in solution. See Eq. (8).	100 μs to 10 ms
$\tau_{\text{DNA}}^{(0)}$	Similar to τ_{DNA} but considered in the limit of uncharged or completely screened ‘‘sticky end’’ molecules. See Eq. (8).	1 μs to 100 μs

- [1] C. A. Mirkin, R. L. Letsinger, R. C. Mucic, and J. J. Storhoff, *Nature* **382**, 607 (1996).
- [2] M. P. Valignat, O. Theodoly, J. C. Crocker, W. B. Russel, and P. M. Chaikin, *Proc. Natl. Acad. Sci. USA* **102**, 4225 (2005).
- [3] P. L. Biancaniello, A. J. Kim, and J. C. Crocker, *Phys. Rev. Lett.* **94**, 058302 (2005).
- [4] S. Y. Park, A. K. R. Lytton-Jean, S. Weigand, G. C. Schatz, and C. A. Mirkin, *Nature* **451**, 553 (2008).
- [5] D. Nykypanchuk, M. M. Maye, D. vander Lelie, and O. Gang, *Nature* **451**, 549 (2008).
- [6] M. M. Maye, D. Nykypanchuk, M. Cuisinier, D. vander Lelie, and O. Gang, *Nat. Mater.* **8**, 388 (2009).
- [7] M. E. Leunissen, R. Dreyfus, R. Sha, T. Wang, N. C. Seeman, D. J. Pine, and P. M. Chaikin, *Soft Matter* **5**, 2422 (2009).
- [8] W. B. Roger and J. C. Crocker, *Proc. Natl. Acad. Sci. USA* **108**, 15687 (2011).
- [9] M. E. Leunissen, R. Dreyfus, F. C. Cheong, D. G. Grier, R. Sha, N. C. Seeman, and P. M. Chaikin, *Nat. Mater.* **8**, 590 (2009).
- [10] R. Dreyfus, M. E. Leunissen, R. Sha, A. V. Tkachenko, N. C. Seeman, D. J. Pine, and P. M. Chaikin, *Phys. Rev. Lett.* **102**, 048301 (2009).
- [11] R. Dreyfus, M. E. Leunissen, R. Sha, A. Tkachenko, N. C. Seeman, D. J. Pine, and P. M. Chaikin, *Phys. Rev. E* **81**, 041404 (2010).
- [12] K.-T. Wu, L. Feng, R. Sha, R. Dreyfus, A. Y. Grosberg, N. C. Seeman, and P. M. Chaikin, *Proc. Natl. Acad. Sci. USA* **109**, 18731 (2012).
- [13] B. M. Mognetti, M. E. Leunissen, and D. Frenkel, *Soft Matter* **8**, 2213 (2012).
- [14] B. M. Mognetti, P. Varilly, S. Angioletti-Uberti, F. J. Martinez-Veracoechea, J. Dobnikar, M. E. Leunissen, and D. Frenkel, *Proc. Natl. Acad. Sci. USA* **109**, E378 (2012).
- [15] W. B. Russel, D. A. Saville, and W. R. Schowalter, *Colloidal Dispersions* (Cambridge University Press, Cambridge, 1999), Chap. 2.
- [16] According to Ref. [15], for a pair of radius $R_p \approx 980$ nm colloids separated by a surface distance $L \approx 16.8$ nm, the diffusion coefficient is reduced by a factor of L/R_p . Hence, the collision time can be estimated as $\frac{L^2}{D(L/R_p)} \approx 30$ ms.
- [17] The Debye screening length is defined as $\lambda \equiv \sqrt{\frac{1}{2} \epsilon k_B T / (q^2 \sum_i n_i Z_i^2)}$, in which ϵ is the dielectric constant of the buffer, q is the elementary charge, and n_i is the density of ion species “ i ” of charge Z_i .
- [18] With no “additional” [NaCl], our buffer still contains the ions from PB and SDS.
- [19] M. von Smoluchowski, *Z. Phys. Chem.* **92**, 129 (1917).
- [20] W. B. Russel, D. A. Saville, and W. R. Schowalter, *Colloidal Dispersions* (Cambridge University Press, Cambridge, 1999), Chap. 8.
- [21] Since there is a slight variation in the viscosity of water, η , with temperature, when comparing data to the model we normalize all times by $D \equiv D_{27^\circ\text{C}}$.
- [22] R. Erban and S. J. Chapman, *Phys. Biol.* **4**, 16 (2007).
- [23] A. P. Washabaugh and M. Zahn, *IEEE Trans. Dielectr. Electr. Insul.* **4**, 688 (1997).
- [24] R. C. Ball, D. A. Weitz, T. A. Witten, and F. Leyvraz, *Phys. Rev. Lett.* **58**, 274 (1987).
- [25] D. A. Weitz, J. S. Huang, M. Y. Lin, and J. Sung, *Phys. Rev. Lett.* **54**, 1416 (1985).
- [26] N.-K. Lee, A. Johner, F. Thalmann, L. Cohen-Tannoudji, E. Bertrand, J. Baudry, J. Bibette, and C. M. Marques, *Langmuir* **24**, 1296 (2008).
- [27] J. Baudry, C. Rouzeau, C. Goubault, C. Robic, L. Cohen-Tannoudji, A. Koenig, E. Bertrand, and J. Bibette, *Proc. Natl. Acad. Sci. USA* **103**, 16076 (2006).
- [28] Y. Zhang, H. Zhou, and Z.-C. Ou-Yang, *Biophys. J.* **81**, 1133 (2001).
- [29] J. R. Wenner, M. C. Williams, I. Rouzina, and V. A. Bloomfield, *Biophys. J.* **82**, 3160 (2002).
- [30] R. Jin, G. Wu, Z. Li, C. A. Mirkin, and G. C. Schatz, *J. Am. Chem. Soc.* **125**, 1643 (2003).
- [31] H. X. Zhou, *Biophys. J.* **64**, 1711 (1993).
- [32] Y. Okahata, M. Kawase, K. Niikura, F. Ohtake, H. Furusawa, and Y. Ebara, *Anal. Chem.* **70**, 1288 (1998).
- [33] See Supplemental Material at <http://link.aps.org/supplemental/10.1103/PhysRevE.88.022304> for further details on the calculation of the barrier U based on various intermediate configurations of DNA hybridization.
- [34] V. A. Bloomfield, D. M. Crothers, and I. Tinoco, *Nucleic Acids: Structures, Properties, and Functions* (University Science Books, Sausalito, California, 2000), Chap. 11.
- [35] A. E. Nkodo, J. M. Garnier, B. Tinland, H. Ren, C. Desruisseaux, L. C. McCormick, G. Drouin, and G. W. Slater, *Electrophoresis* **22**, 2424 (2001).
- [36] G. Balgi, D. E. Leckband, and J. M. Nitsche, *Biophys. J.* **68**, 2251 (1995).
- [37] S. Bennett, *IEEE Control Syst. Mag.* **4**, 10 (1984).